

Influences of Dynamic Moving Forces on the Functionally Graded Porous-Nonuniform Beams

Nguyen Dinh Kien¹, Tran Thi Thom¹, Buntara Sthenly Gan^{2,*}, Bui Van Tuyen³

¹Department of Solid Mechanics, Institute of Mechanics, VAST, Hanoi, Vietnam.

²Department of Architecture, College of Engineering, Nihon University, Koriyama, Japan.

³Department of Mechanical Engineering, ThuyLoi University, Dong Da, Hanoi, Vietnam.

Received 02 March 2016; received in revised form 15 June 2016; accepted 17 June 2016

Abstract

The dynamic response of functionally graded (FG) porous-nonuniform beams subjected to moving forces is investigated. The beam cross-section is assumed to vary longitudinally in the width direction by a linear or quadratic function. A modified rule of mixture, taking the effect of porosities into account, is adopted in evaluating the effective material properties. Based on Timoshenko beam theory, governing equations of motion are derived from Hamilton's principle, and they are solved by a finite element model. The dynamic response of a simply supported FG porous beam is computed with the aid of the Newmark method. The validation of the derived formulation is confirmed by comparing the obtained numerical results with the data available in the literature. A parametric study is conducted to highlight the effect of the material inhomogeneity, porosity volume fraction, section profile and loading parameters on the dynamic behavior of the beams.

Keywords: functionally graded material, porous-nonuniform beam, porosity, dynamic analysis, finite element model

1. Introduction

The problems of elastic beams under moving loads are often met in practice, and they are subject of investigation for a long time. Both analytical and numerical methods are widely employed in solving the moving load problems. Frýba [1] presented a large number of closed-form solutions for elastic beams under different types of moving loads. The traditional two-node finite beam model was used by Lin and Trethewey [2] to investigate the dynamic response of Euler-Bernoulli beams subjected to moving spring-mass-damper system. Also using the finite element method, Thambiratnam and Zhuge [3] computed the dynamic response of beams on an elastic foundation subjected to multiple moving forces. The discrete element method was employed by Ziaei-Rad, Ariaei and Imregun [4] to study the dynamic behavior of Timoshenko beams under uniform partially distributed moving masses. Moghaddas, Sedaghati and Esmailzadeh [5] studied the dynamic response of a bridge under a vehicle by modelling the bridge as a simply supported Timoshenko beam and the vehicle as a half-car planner model. Also modelling a bridge as a Timoshenko beam, Moghaddas, Esmailzadeh, Sedaghati and Khosravi [6] developed an algorithm for determining the optimum values of a mass damper attached to the bridge for reducing its mid-span deflection. Based on eigenfunction expansion method, Roshandel, Mofid and Ghannadiasl [7] studied the dynamic response of nonuniform beams subjected to a moving mass.

*Corresponding author. E-mail address: buntara@arch.ce.nihon-u.ac.jp

Tel.: +81-24-9568375; Fax: +81-24-956-8375

Functionally graded materials (FGMs) have received much attention from engineers and researchers since Japanese scientists in mid-1980s first initiated them, Koizumi [8]. FGMs are produced by the continuously varying volume fraction of constituent materials, usually ceramics and metals, in one or more predefined directions. As a result, the properties of FGMs exhibit continuous change and thus eliminating many undesired problems like delamination and stress concentrations as in conventional composites. FGMs have wide applications, including aerospace structures, turbine blades, and rocket engine components, Jha, Kant and Singh [9]. Many investigations on analysis of functionally graded (FG) structures can be found in the literature, contributions that are closely related to the present work are discussed herein.

The Timoshenko beam theory was used by Chakraborty, Gopalakrishnan and Reddy [10] in the derivation of finite element formulation for investigating the thermoelastic behavior of FG beams. Kadoli, Akhtar and Ganesan [11] performed a static investigation of FG beams by deriving a third-order finite element formulation. Alshorbagy, Eltaher and Mahmoud [12] used a simple two-node beam element to compute the natural frequencies of FG Euler-Bernoulli beams. The finite element method has also been employed by Shahba, Attarnejad, Marvi and Hajilar [13] in studying the free vibration of tapered axially FG Timoshenko beams. Nguyen [14,15], Nguyen and Gan [16] developed the co-rotational finite element formulations for studying the large displacements of tapered FG beams subjected to end forces. The analysis of FG beams under moving loads was carried out by some researchers recently. Among them, Şimşek and Kocatürk [17] employed the Lagrange multiplier method to solve the equations of motion of FG beams under a moving harmonic force. Also using the Lagrange multiplier method, Şimşek investigated the dynamic analysis of FG beams subjected to a moving mass [18], and a nonlinear FG beam under a moving harmonic force [19]. The differential quadrature method was used in combination with Newmark method by Khalili, Jafari and Eftekhari [20] in the computation of the dynamic deflection of FG beams. Rajabi, Kargarnovin and Gharini [21] employed Runge-Kutta method to study the dynamic behavior of an FG Euler-Bernoulli beam subjected to a moving oscillator. The finite element method was used by Nguyen, Gan and Le [22], Le, Gan, Trinh and Nguyen [23], Gan, Trinh, Le and Nguyen [24] to compute the dynamic characteristics of FG beams subjected to moving forces.

The effect of porosities on the mechanical behaviour of FG structures was considered in recent years. Wattanasakulpong and Ungbhakorn [25], Wattanasakulpong and Chaikittiratana [26] modified the rule of mixture for taking porosities into consideration in their investigation of free vibration of FG beams. Chen, Yang and Kitipornchai [27] employed the Ritz method to obtain expressions for the critical load and bending deflection of Timoshenko beams made of porous FGM. Atmane, Tounsi and Bernard [28] presented a shear and normal deformation beam theory for thick FG beams with porosities and then applied it to study the free vibration of FG beams resting on a two-parameter elastic foundation. The large amplitude vibration of porous FG beams was investigated by Ebrahimi and Zia [29] by using the Galerkin and multiple scales methods. The differential transform method was used by Ebrahimi, Ghasemi and Salari [30] to study the free vibration of FG porous Euler-Bernoulli beams in a thermal environment.

To the authors' best knowledge, the dynamic response of nonuniform FG porous beams subjected to multiple moving forces has not been investigated in the literature, and it will be studied in the present work for the first time. The beam cross-section considered herein is assumed to vary longitudinally in the width direction by a linear or quadratic function. The modified rule of the mixture is adopted in the evaluation of the effective material properties. Based on Timoshenko beam theory, equations of motion for the beam are derived from Hamilton's principle, and they are solved by a finite element model. The dynamic response of a simply supported FG porous beam is computed by using an implicit Newmark method. A parametric study is carried out to highlight the effect of the material distribution, volume fraction of porosity and loading parameters on the dynamic response of the beam. The influence of the section profile and the aspect ratio on the dynamic behaviour of the beam is also studied and discussed.

2. Porous-Nonuniform FG Beams

A simply supported beam with length of L , under N forces P_1, P_2, \dots, P_N , moving from left to right with a speed v , as depicted in Fig. 1 is considered. The beam cross-section is assumed to be rectangular with constant height (h). A Cartesian coordinate system (x, z) is introduced as that the x -axis lies on the mid-plane, and the z -axis directs upward. The distance between the forces (d) and the speed of the forces (v) are considered to be constant in the present work.

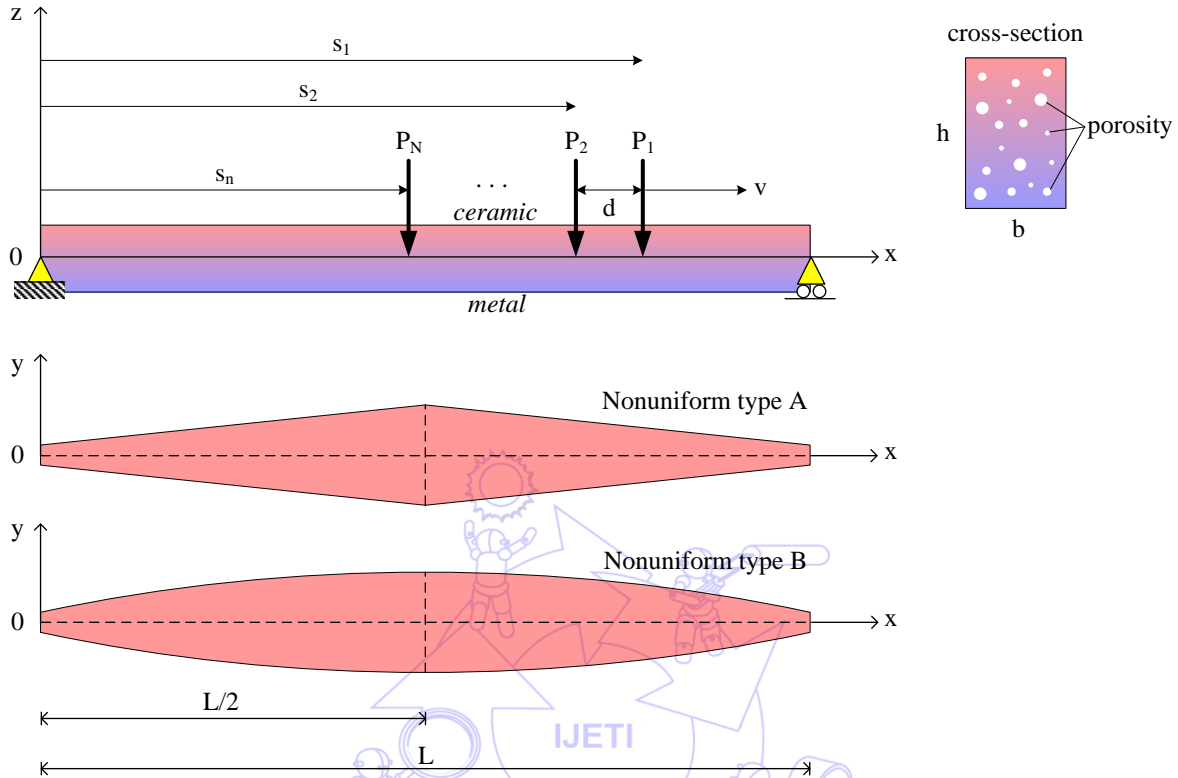


Fig. 1 Nonuniform FG porous beam subjected to moving forces

The beam width (b) is assumed to vary longitudinally in two following types

$$\text{Type A: } b(x) = b_0 \left(1 - \beta \left| \frac{x}{L} - \frac{1}{2} \right| \right); \quad \text{Type B: } b(x) = b_0 \left[1 - \beta \left(\frac{x}{L} - \frac{1}{2} \right)^2 \right] \quad (1)$$

where b_0 is width of the mid-span cross-section, and $\beta (0 \leq \beta < 2)$ is the section parameter. When $\beta=0$, the beam becomes uniform. The above linear and quadratic variations of the section profile are depicted in the lower part of Fig. 1.

The beam material is assumed to be composed of metal and ceramic whose volume fraction varies in the transverse direction according to

$$V_c = \left(\frac{z}{h} + \frac{1}{2} \right)^n, \quad V_m + V_c = 1 \quad (2)$$

where V_c and V_m are the volume fractions of ceramic and metal, respectively; $n (0 \leq n < \infty)$ is the grading index which dictates the variation of the constituents through the beam thickness. As seen from Eq. (2), the bottom surface (according to $z = -h/2$) contains only metal, and the top surface ($z = h/2$) is pure ceramic. In Eq. (2) and hereafter, the subscripts 'c' and 'm' are used to indicate 'ceramic' and 'metal', respectively.

To account for porosities, the modified rule of mixture introduced in [25] is adopted herein

$$\mathcal{P} = \mathcal{P}_c \left(V_c - \frac{\alpha}{2} \right) + \mathcal{P}_m \left(V_m - \frac{\alpha}{2} \right) \quad (3)$$

where \mathcal{P} is the effective property of the FGM; \mathcal{P}_m and \mathcal{P}_c are respectively the properties of metal and ceramic; α ($\alpha < 1$) is the porosity volume fraction. From Eqs. (2) and (3), the effective Young's modulus $E(z)$, shear modulus $G(z)$, and mass density $\rho(z)$ of the FG porous beam are given by

$$\begin{aligned} E(z) &= (E_c - E_m) \left(\frac{z}{h} + \frac{1}{2} \right)^n + E_m - \frac{\alpha}{2} (E_c + E_m) \\ G(z) &= (G_c - G_m) \left(\frac{z}{h} + \frac{1}{2} \right)^n + G_m - \frac{\alpha}{2} (G_c + G_m) \\ \rho(z) &= (\rho_c - \rho_m) \left(\frac{z}{h} + \frac{1}{2} \right)^n + \rho_m - \frac{\alpha}{2} (\rho_c + \rho_m) \end{aligned} \quad (4)$$

when $\alpha=0$, Eg. (4) deduces to the well-known expressions for the effective properties of FG perfect (without porosities) beams [10,11].

3. Analysis of FG Beams Under Moving Forces

Based on Timoshenko beam theory, the displacements of an arbitrary point along the x and z -axes, u_1 and u_3 , respectively are given by

$$\begin{aligned} u_1(x, z, t) &= u(x, t) - z\theta(x, t) \\ u_3(x, z, t) &= w(x, t) \end{aligned} \quad (5)$$

where t is the time; $u(x, t)$ and $w(x, t)$ are respectively the axial and transverse displacements of the point on the x -axis, and $\theta(x, t)$ is the cross-section rotation. The axial strain (ϵ_{xx}) and shear strain (γ_{xz}) resulted from Eg. (5) are

$$\epsilon_{xx} = u_{,x} - z\theta_{,x}, \quad \gamma_{xz} = w_{,x} - \theta \quad (6)$$

where $(.)_{,x}$ denotes the derivative with respect to x . In Eg. (6) and hereafter, the variables x and t are omitted from the displacements and rotation for the sake of simplicity.

Based on Hooke's law, the axial stress (σ_{xx}) and the shear stress (τ_{xz}) associated with the axial and shear strains are given by

$$\sigma_{xx} = E(z)(u_{,x} - z\theta_{,x}), \quad \tau_{xz} = \psi G(z)(w_{,x} - \theta) \quad (7)$$

with ψ is the correction factor, chosen by $5/6$ for the beam with rectangular cross-section [18].

From Eqs. (6) and (7) one can write the strain energy (U) of the beam in the form

$$U = \frac{1}{2} \int_0^L \left[A_{11} u_{,x}^2 - 2A_{12} u_{,x} \theta_{,x} + A_{22} \theta_{,x}^2 + \psi A_{33} (w_{,x} - \theta)^2 \right] dx \quad (8)$$

In the above Eq., A_{11} , A_{12} , A_{22} and A_{33} are respectively the extensional, extensional-bending coupling, bending and shear rigidities, defined as follows

$$(A_{11}, A_{12}, A_{22}) = \int_{A(x)} E(z) (1, z, z^2) dA, \quad A_{33} = \int_{A(x)} G(x) dA \quad (9)$$

The rigidities in Eq. (9) can be written in explicit forms as

$$\begin{aligned} A_{11} &= b(x)h \left[\frac{1}{(n+1)} (E_c + nE_m) - \frac{\alpha}{2} (E_c + E_m) \right] \\ A_{12} &= b(x)h^2 \frac{n}{2(n+1)(n+2)} (E_c - E_m) \\ A_{22} &= b(x)h^3 \left[\frac{(n^2 + n + 2)}{4(n+1)(n+2)(n+3)} (E_c - E_m) + \frac{1}{12} E_m - \frac{\alpha}{24} (E_c + E_m) \right] \\ A_{33} &= b(x)h \left[\frac{1}{(n+1)} (G_c + nG_m) - \frac{\alpha}{2} (G_c + G_m) \right] \end{aligned} \quad (10)$$

The kinetic energy of the beam (T) resulted from Eq. (5) is as follows

$$T = \frac{1}{2} \int_0^L \left[I_{11} (\dot{u}^2 + \dot{w}^2) - 2I_{12} \dot{u} \dot{\theta} + I_{22} \dot{\theta}^2 \right] dx \quad (11)$$

where an overdot denotes differentiation with respect to time; I_{11} , I_{12} and, I_{22} are the mass moments, defined as

$$(I_{11}, I_{12}, I_{22}) = \int_{A(x)} \rho(z) (1, z, z^2) dA \quad (12)$$

The explicit forms for the mass moments are as follows

$$\begin{aligned} I_{11} &= b(x)h \left[\frac{1}{(n+1)} (\rho_c + n\rho_m) - \frac{\alpha}{2} (\rho_c + \rho_m) \right] \\ I_{12} &= b(x)h^2 \frac{n}{2(n+1)(n+2)} (\rho_c - \rho_m) \\ I_{22} &= b(x)h^3 \left[\frac{(n^2 + n + 2)}{4(n+1)(n+2)(n+3)} (\rho_c - \rho_m) + \frac{1}{12} \rho_m - \frac{\alpha}{24} (\rho_c + \rho_m) \right] \end{aligned} \quad (13)$$

The potential of the moving forces (V) is simply given by

$$V = - \sum_{i=1}^N P_i w(x, t) \delta(s_i - vt_i) \quad (14)$$

with $\delta(\cdot)$ is the delta Dirac function; s_i is the current position of load P_i with respect to the left end, and t_i is the travelling time of the load P_i , measured from the time when this load enters the beam.

Applying Hamilton's principle to Egs. (8), (11) and (14), one can obtain the following equations of motion for the beam as

$$\begin{cases} I_{11}\ddot{u} - I_{12}\ddot{\theta} - (A_{11}u_{,x})_{,x} + (A_{12}\theta_{,x})_{,x} = 0 \\ I_{11}\ddot{w} - \psi[A_{33}(w_{,x} - \theta)]_{,x} = \sum_{i=1}^N P_i \delta(s_i - vt_i) \\ I_{22}\ddot{\theta} - I_{12}\ddot{u} + (A_{12}u_{,x})_{,x} - (A_{22}\theta_{,x})_{,x} - \psi A_{33}(w_{,x} - \theta) = 0 \end{cases} \quad (15)$$

and, the non-essential boundary conditions

$$\begin{aligned} A_{11}u_{,x} - A_{12}\theta_{,x} &= \bar{N}, \quad A_{22}\theta_{,x} - A_{12}u_{,x} = \bar{M}, \\ \psi A_{33}(w_{,x} - \theta) &= \bar{Q} \quad \text{at } x=0 \text{ and } x=L \end{aligned} \quad (16)$$

In Eg. (16), \bar{N} , \bar{M} and \bar{Q} are the prescribed axial forces, moments and shear forces at the beam ends, respectively. The essential boundary conditions for the simply supported beam in Fig. 1 are

$$u(x,t) = 0 \text{ at } x=0, \quad w(x,t) = 0 \text{ at } x=0 \text{ and } x=L \quad (17)$$

Due to the longitudinal variation of the beam cross-section, the coefficients of the differential Egs. (15) are functions of x , and a closed-form solution is difficult to derive. Here, a finite element model is used for solving Eg. (1). To this end, the beam is assumed to be divided into a number of two-node beam elements with a length of l . The vector of nodal displacements (\mathbf{d}) for a generic element (i, j) has six components as

$$\mathbf{d} = \{u_i \quad w_i \quad \theta_i \quad u_j \quad w_j \quad \theta_j\}^T \quad (18)$$

where u_i , w_i and θ_i are respectively the axial, transverse displacements and rotation at node i , and u_j , w_j and θ_j are the corresponding quantities at node j . In Eg. (18) and hereafter a superscript ' T ' denotes the transpose of a vector or a matrix.

The displacements u , w and rotation θ are interpolated from the nodal displacements according to

$$u = \mathbf{N}_u \mathbf{d}, \quad w = \mathbf{N}_w \mathbf{d}, \quad \theta = \mathbf{N}_\theta \mathbf{d} \quad (19)$$

where $\mathbf{N}_u = \{N_{u1} \ N_{u2} \ \dots \ N_{u6}\}$, $\mathbf{N}_w = \{N_{w1} \ N_{w2} \ \dots \ N_{w6}\}$, $\mathbf{N}_\theta = \{N_{\theta1} \ N_{\theta2} \ \dots \ N_{\theta6}\}$ are the matrices of shape functions for u , w and θ , respectively.

The shape functions of the present work are obtained by solving the static part of the Eg. (15) for a uniform beam segment. In this case, the equilibrium Egs. have the same form as that of the FG perfect Timoshenko beam, and they lead to the following shape functions [10,23]

$$\begin{aligned} N_{u1} &= \frac{l-x}{l}, \quad N_{u2} = \frac{6\lambda}{(1+\phi)} \left[\left(\frac{x}{l}\right)^2 - \left(\frac{x}{l}\right) \right], \quad N_{u3} = \frac{3\lambda}{(1+\phi)} \left[\left(\frac{x}{l}\right)^2 - \left(\frac{x}{l}\right) \right] \\ N_{u4} &= \frac{x}{l}, \quad N_{u5} = -\frac{6\lambda}{(1+\phi)} \left[\left(\frac{x}{l}\right)^2 - \left(\frac{x}{l}\right) \right], \quad N_{u6} = N_{u3} \end{aligned} \quad (20)$$

$$\begin{aligned}
N_{w1} &= N_{w4} = 0 \\
N_{w2} &= \frac{1}{(1+\phi)} \left[2\left(\frac{x}{l}\right)^3 - 3\left(\frac{x}{l}\right)^2 - \phi\left(\frac{x}{l}\right) + (1+\phi) \right] \\
N_{w3} &= \frac{l}{(1+\phi)} \left[\left(\frac{x}{l}\right)^3 - \left(2 + \frac{\phi}{2}\right)\left(\frac{x}{l}\right)^2 + \left(1 + \frac{\phi}{2}\right)\left(\frac{x}{l}\right) \right] \\
N_{w5} &= -\frac{1}{(1+\phi)} \left[2\left(\frac{x}{l}\right)^3 - 3\left(\frac{x}{l}\right)^2 - \phi\left(\frac{x}{l}\right) \right] \\
N_{w6} &= \frac{l}{(1+\phi)} \left[\left(\frac{x}{l}\right)^3 - \left(1 - \frac{\phi}{2}\right)\left(\frac{x}{l}\right)^2 - \frac{\phi}{2}\left(\frac{x}{l}\right) \right]
\end{aligned} \tag{21}$$

and

$$\begin{aligned}
N_{\theta1} &= N_{\theta4} = 0, \\
N_{\theta2} &= \frac{6}{l(1+\phi)} \left[\left(\frac{x}{l}\right)^2 - \left(\frac{x}{l}\right) \right], \quad N_{\theta3} = \frac{1}{(1+\phi)} \left[3\left(\frac{x}{l}\right)^2 - (4+\phi)\left(\frac{x}{l}\right) + (1+\phi) \right] \\
N_{\theta5} &= -\frac{6}{l(1+\phi)} \left[\left(\frac{x}{l}\right)^2 - \left(\frac{x}{l}\right) \right], \quad N_{\theta6} = \frac{1}{(1+\phi)} \left[3\left(\frac{x}{l}\right)^2 - (2-\phi)\left(\frac{x}{l}\right) \right]
\end{aligned} \tag{22}$$

with

$$\lambda = \frac{A_{12}}{A_{11}}, \quad \phi = \frac{12}{l^2} \left(\frac{A_{22}}{\psi A_{33}} - \frac{A_{12}}{A_{11}} \right) \tag{23}$$

For homogeneous beams $A_{12}=0$ and $\phi=12EI/(l^2 \psi GA)$, with EI and GA are the bending stiffness and shear stiffness, respectively. In this case, the expressions for bending shape functions, Eqs. (21) and (22), deduce exactly to the ones, previously derived by Kosmatka [31] for a uniform, homogenous Timoshenko beam. For the variable cross-section considered herein, both λ and ϕ are functions of x , and even in this case, one can easily verify that the shape functions in Eqs. (19)-(22) satisfy the following element end conditions

$$\begin{aligned}
u &= u_i, \quad w = w_i, \quad \theta = \theta_i \quad \text{when } x = 0 \\
u &= u_j, \quad w = w_j, \quad \theta = \theta_j \quad \text{when } x = l
\end{aligned} \tag{24}$$

For the sake of simplicity, the present work uses the area and moment of inertia of the cross-section at the left node of the element to calculate the parameters λ and ϕ in Eqs. (19)-(22).

Using the above shape functions, one can write the strain and kinetic energies for the beam in the form

$$U = \sum_{e=1}^{ne} \mathbf{d}_e^T \mathbf{k}_e \mathbf{d}_e, \quad T = \sum_{i=1}^{n_d} \dot{\mathbf{d}}_e^T \mathbf{m}_e \dot{\mathbf{d}}_e \tag{25}$$

where ne is the total number of elements; \mathbf{k} and \mathbf{m} are respectively the element stiffness and consistent mass matrices with the following forms

$$\mathbf{k} = \int_0^l \left[\mathbf{N}_{u,x}^T A_{11} \mathbf{N}_{u,x} - \mathbf{N}_{u,x}^T A_{12} \mathbf{N}_{\theta,x} + \mathbf{N}_{\theta,x}^T A_{22} \mathbf{N}_{\theta,x} + (\mathbf{N}_{w,x}^T - \mathbf{N}_{\theta}^T) \psi A_{33} (\mathbf{N}_{w,x} - \mathbf{N}_{\theta}) \right] dx \tag{26}$$

and

$$\mathbf{m} = \int_0^l \left(\mathbf{N}_u^T I_{11} \mathbf{N}_u + \mathbf{N}_w^T I_{11} \mathbf{N}_w - \mathbf{N}_u^T I_{12} \mathbf{N}_{\theta} + \mathbf{N}_{\theta}^T I_{22} \mathbf{N}_{\theta} \right) dx \tag{27}$$

Having the element stiffness and mass matrices derived, the finite element equation for dynamic analysis of the beam ignoring the damping effect can be written in the following form

$$\mathbf{M}\ddot{\mathbf{D}} + \mathbf{K}\mathbf{D} = \mathbf{F}_{ex} \tag{28}$$

where \mathbf{D} , \mathbf{M} , \mathbf{K} are the structural nodal displacement vector, mass and stiffness matrices, obtained by assembling the element displacement vector \mathbf{d} , mass matrix \mathbf{m} and stiffness matrix \mathbf{k} over the all elements, respectively; \mathbf{F}_{ex} is the structural nodal load vector with the following form

$$\mathbf{F}_{ex} = \left\{ \begin{matrix} 0 \dots \underbrace{P_N \mathbf{N}_w |_{x_N}}_{\text{loading element}} \dots 0 \dots \underbrace{P_i \mathbf{N}_w |_{x_i}}_{\text{loading element}} \dots 0 \dots \underbrace{P_1 \mathbf{N}_w |_{x_1}}_{\text{loading element}} \dots 0 \end{matrix} \right\}^T \tag{29}$$

The above nodal load vector contains all zero coefficients, except for the elements currently under loading. The notation $\mathbf{N}_w |_{x_i}$ in Eg. (29) means that the shape functions \mathbf{N}_w are evaluated at the abscissa x_i ($i=1 \dots N$), the current position of the load P_i on the left node of the element. The system of Eqs. (28) can be solved by the direct integration Newmark method. The average acceleration method described by Géradin and Rixen [32], which ensures the unconditional convergence is adopted in the present work. In the free vibration analysis, the right-hand side of Eg. (28) is set to zeros, and a harmonic response, $\mathbf{D} = \bar{\mathbf{D}} \sin \omega t$, is assumed, so that Eg. (28) deduces to

$$(\mathbf{K} - \omega^2 \mathbf{M}) \bar{\mathbf{D}} = \mathbf{0} \tag{30}$$

where ω is the circular frequency, and $\bar{\mathbf{D}}$ is the vibration amplitude. Eg. (30) leads to an eigenvalue problem, and its solution can be obtained by the standard method. To improve the accuracy of numerical results, the exact variation of the beam width is given by Eg. (1) is employed in the evaluation of the element stiffness and mass.

4. Numerical Results and Discussion

The dynamic response of FG porous beams under moving forces is numerically studied in this Section. Otherwise mentioned, a simply supported beam with an aspect ratio $L/h=20$ subjected to three moving forces with uniform amplitude, $P_1=P_2=P_3=P=100$ kN, is considered. The beam is assumed initially at rest, and it is formed from Aluminum (Al) and Alumina (Al_2O_3) with the following data [18]: $E_m=70\text{GPa}$, $\rho_m=2702$ kg/m³ and $\nu_m=0.23$ for Al; $E_c=380\text{GPa}$, $\rho_c=3800$ kg/m³ and $\nu_c=0.23$ for Al_2O_3 . A uniform increment time step, $\Delta t = \Delta T/500$, where $\Delta T = L/v$ is the total time necessary for a single force to cross the beam, is employed for the Newmark method. As in case of homogeneous beams, the following dimensionless parameter is introduced

$$f_D = \max \left(\frac{w(L/2, t)}{w_0} \right) \tag{31}$$

where $w_0 = PL^3/48E_m I_0$ is the maximum static deflection of the uniform Al beam. The parameter f_D in (31) is defined in the same way as the Dynamic Amplification Factor (DAF) in the moving load problem of homogeneous beams [1], and it is also called the DAF herein.

Table 1 Comparison of dimensionless fundamental frequency ($\bar{\omega}$) of the clamped FG beam.

α	L/h	Source	$n=0.2$	$n=0.5$	$n=1$	$n=2$	$n=5$
0 (Perfect)	5	[26]	1.8823	1.7392	1.5844	1.4417	1.3328
		Present	1.8772	1.7351	1.5814	1.4393	1.3300
	10	[26]	1.0884	0.9992	0.9056	0.8255	0.7782
		Present	1.0875	0.9987	0.9055	0.8258	0.7782
	20	[26]	0.5691	0.5213	0.4716	0.4302	0.4085
		Present	0.5690	0.5212	0.4716	0.4303	0.4086
0.2 (Porous)	5	[26]	1.9205	1.7402	1.5210	1.2815	1.0933
		Present	1.9155	1.7364	1.5190	1.2810	1.0928
	10	[26]	1.1092	0.9956	0.8606	0.7193	0.6229
		Present	1.1083	0.9953	0.8603	0.7194	0.6230
	20	[26]	0.5797	0.5186	0.4465	0.3722	0.3241
		Present	0.5796	0.5184	0.4467	0.3725	0.3244

Before computing the dynamic response, the accuracy of the formulation is verified. To this end, the fundamental frequency of a clamped uniform FG perfect and porous beams composed of Al and Al_2O_3 is firstly computed. In Table 1, the dimensionless fundamental frequency ($\bar{\omega}$) is listed for various values of the index n and the aspect ratio L/h , where the results in [26] by using Chebyshev collocation method are also given. In Table 1, $\bar{\omega}$ is defined as follows

$$\bar{\omega} = \omega L \sqrt{\rho_m / E_m} \tag{32}$$

where ω is the fundamental frequency. Good agreement between the result of the present work with that in [26], regardless of the aspect ratio and the porosity volume fraction is noted from Table 1.

Table 2 Comparison of maximum DAF and corresponding speed of uniform FGM beam

	Source	$n=0.2$	$n=0.5$	$n=1$	$n=2$	Pure Al	Pure Al_2O_3
max(DAF)	Present	1.0402	1.1505	1.2566	1.3446	1.7420	0.9380
	[17]	1.0344	1.1444	1.2503	1.3376	1.7324	0.9328
v (m/s)	Present	222	197	178	163	131	251
	[17]	222	198	179	164	132	252

To verify the formulation in evaluating the dynamic response of FG beams, the maximum DAF and the corresponding moving speed of a simply supported uniform FG perfect beam under a moving force, previously studied by in [17] are computed, and the results are given in Table 2. The beam with length $L=20m$, height $h=0.9m$ and width $b=0.4m$, composed of Steel and Alumina in [17] was adopted in assessing the computation. The results in the table were obtained by consideration of the moving speed in the range of 1 m/s to 300 m/s with an increment of 1 m/s, as suggested in [17]. Good agreement between the numerical result of the present work with that of [17] is seen from Table 2.

To verify the formulation in handling multiple moving forces, the dynamic mid-span deflection of a uniform homogeneous perfect beam traversed by three moving forces, previously studied by Henchi, Fafard, Dhatt and Talbot [33] by the dynamic stiffness method, is computed. The data for the computation are as follows: $L = 24.384$ m, $A=0.954$ m², $I = 2.9 \times 10^{-4}$ m⁴, $E = 19 \times 10^{11}$ N/m², $\rho A = 9.576 \times 10^3$ kg/m³. Fig. 2 shows the dynamic mid-span deflection for $P = 5324.256$ N, $v = 22.5$ m/s, $d = L/4$, where the numerical result obtained in [33] is illustrated by small circles. Very good agreement between the numerical results of the present work with that in [33] is seen from Fig. 2. It should be noted that twenty elements have been used in the verification examples, and no improvement in the numerical results was seen for the mesh of more twenty elements.

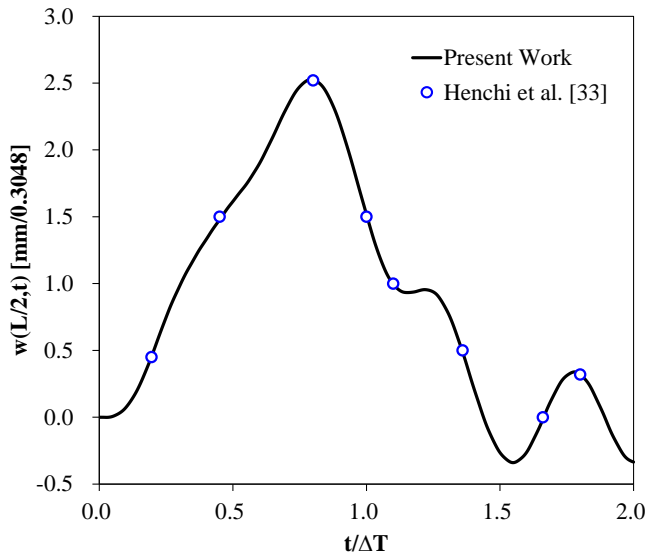
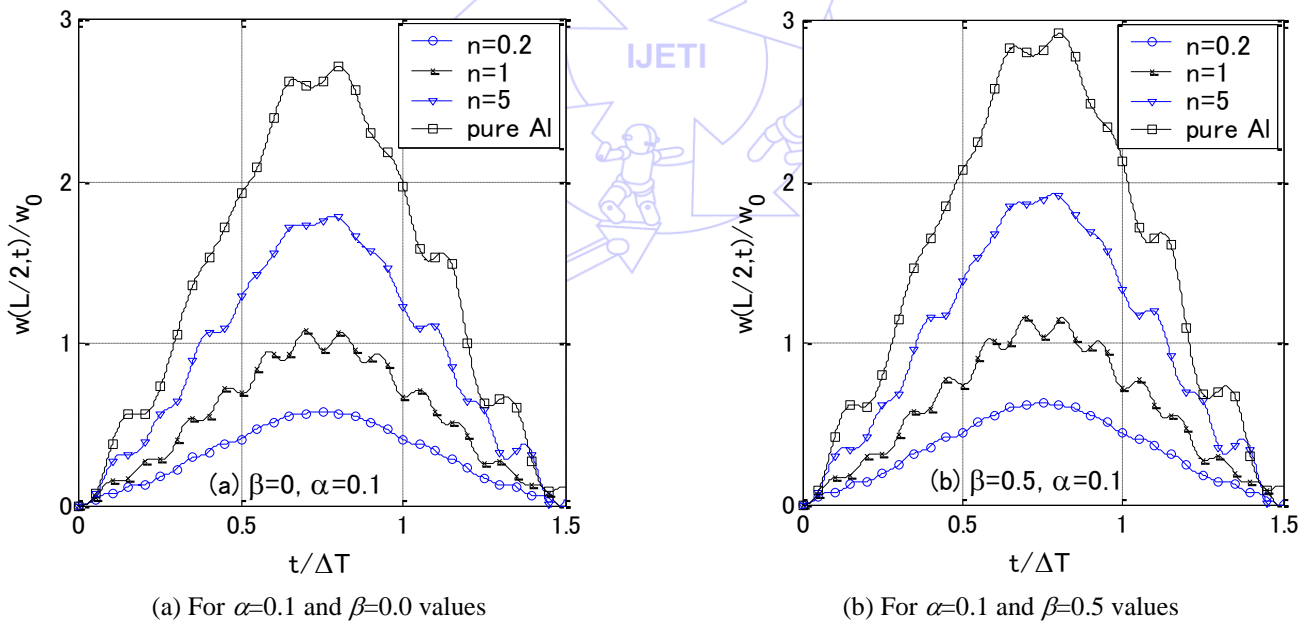


Fig. 2 Dynamic mid-span deflection of uniform homogeneous beam under three moving forces ($d = L/4$, $v = 22.5$ m/s)



(a) For $\alpha=0.1$ and $\beta=0.0$ values

(b) For $\alpha=0.1$ and $\beta=0.5$ values

Fig. 3 Dynamic mid-span deflection of type A beam with different indexes n ($v=20$ m/s, $d=L/4$)

In Fig. 3, the dynamic mid-span deflection of the type A beam having $\alpha=0.1$ under the moving forces with $v=20$ m/s and $d=L/4$ is depicted for various values of the index n and two values of the section parameter, $\beta = 0$ and $\beta = 0.5$. As seen from the figure, the material inhomogeneity strongly affects the dynamic behaviour of the beam. At a given value of the moving speed and distance between the forces, the maximum dynamic mid-span deflection of the beam steadily increases when raising the index n . Furthermore, the beam associated with a higher index n executes less number of vibration cycles, regardless of the section parameter β . The higher dynamic mid-span deflection and the less executed vibration cycles of the beam associated

with a higher index n can be explained by the fact that, as seen from Eg. (4), the beam with a higher index n contains more metal and thus it is softer. In addition, the ratio of the given moving speed to the critical speed, v/v_{cr} , of the softer beam is higher since the critical speed v_{cr} is proportional to the fundamental frequency [1]. As stated by Olsson [34] that the higher v/v_{cr} ratio is the less vibration cycles the beam executes.

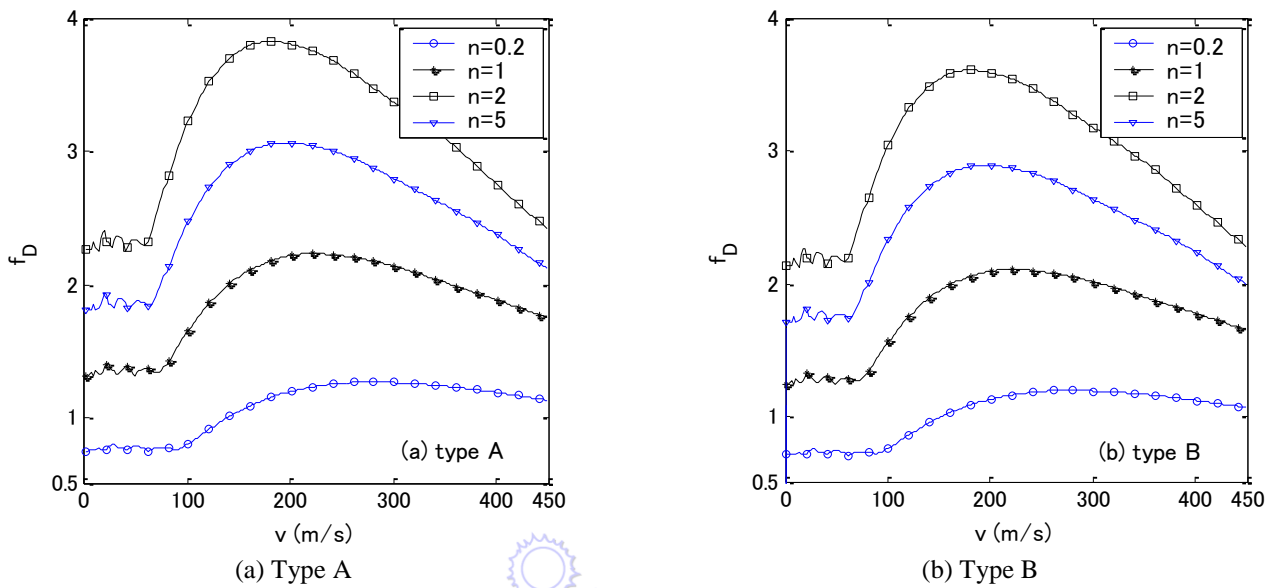


Fig. 4 Relation between DAF and moving speed of FG porous beam with different indexes n ($\alpha=0.1, \beta=0.5, d=L/8$)

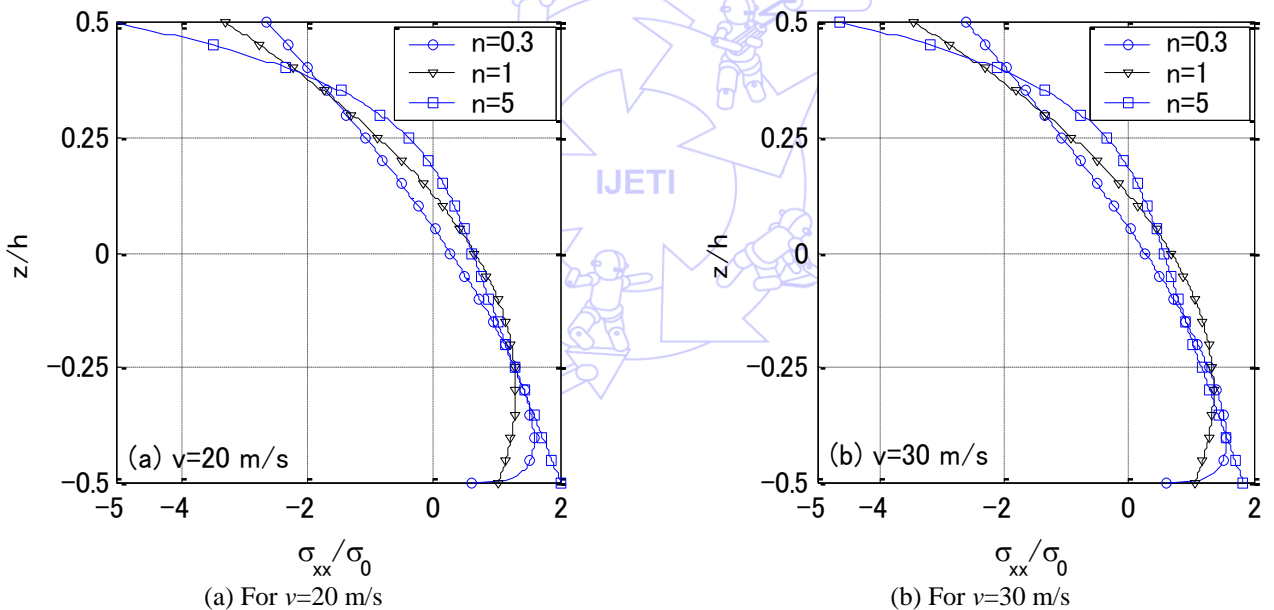


Fig. 5 Thickness distribution of axial stress at mid-span section of type A beam ($\beta=0.5, \alpha=0.1, d=L/4$)

The effect of the material inhomogeneity on the dynamic response of the FG porous beam is also seen from Fig. 4, where the relation between the DAF and the moving speed of both the type A and type B beams is illustrated for various values of the index n and for $\alpha = 0.1, \beta = 0.5, d = L/8$. Regardless of the moving speed and the section profile, the DAF remarkably increases by raising the index n . The section profile slightly changes the magnitude of DAF, but it hardly affects the relation between this factor and the moving speed.

In Fig. 5, the distribution of the axial stress in the thickness direction of mid-span section of the type A beam with $\alpha = 0.1, \beta = 0.5$ is depicted for different grading indexes n and two values of the moving speed, $v=20$ m/s and $v=30$ m/s. The axial stress in the figure was computed at the time when the second force arrives at the mid-span, and it was normalized by the maximum axial stress of a uniform beam under static force P , that is $\sigma_0 = PLh/8I_0$. The axial stress of the FG porous beam is

not symmetric on the original of the coordinate system, and the stress amplitude in the upper half (ceramic-rich) part of the beam is considerably higher than that of the lower (metal-rich) part. Also, the axial stress does not vanish at the mid-plane as in the case of homogeneous beams. Both the stress amplitude and stress distribution of the FG porous beam are greatly influenced by the grading index n . The moving speed v slightly changes the stress amplitude, but it hardly alters the distribution of the axial stress.

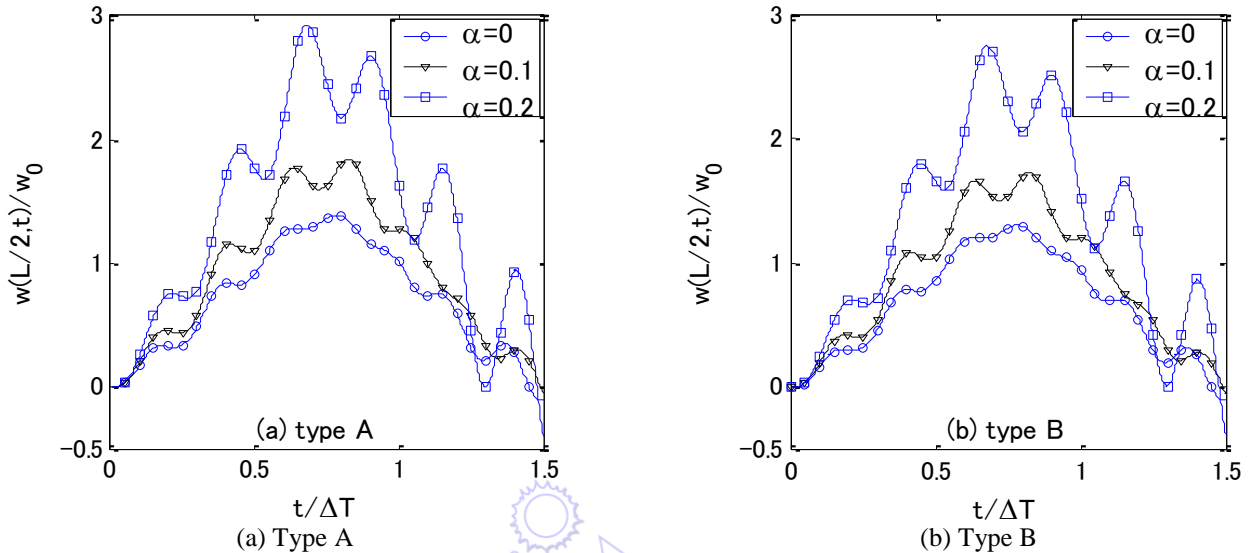


Fig. 6 Dynamic mid-span deflection of FG beam with different porosity volume fractions ($n=3, \beta=0.5, d=L/4, v=30$ m/s)

The dynamic mid-span deflection of both two types of the FG beam with $n=3$ is shown in Fig. 6 for different porosity volume fractions and for $v=30$ m/s, $d=L/4$. As seen from the figure, the dynamic mid-span deflection of the beam is strongly influenced by the porosity volume fraction. For most of the travelling time, the dynamic mid-span deflection is larger for the beam associated with a higher porosity volume fraction. The number of vibration cycles which the beam executes tends to decrease as an increase in the porosity volume fraction. The effect of the porosity volume fraction on the dynamic response of the beam is similar to that of the index n as discussed above, and it can also be explained by the decrease of the rigidities and the fundamental frequency of the beam with a higher porosity volume fraction. The dynamic mid-span deflection of the type B beam is slightly smaller than that of the type A beam, but the relation between the deflection and the time is almost the same for both the types of section profile.

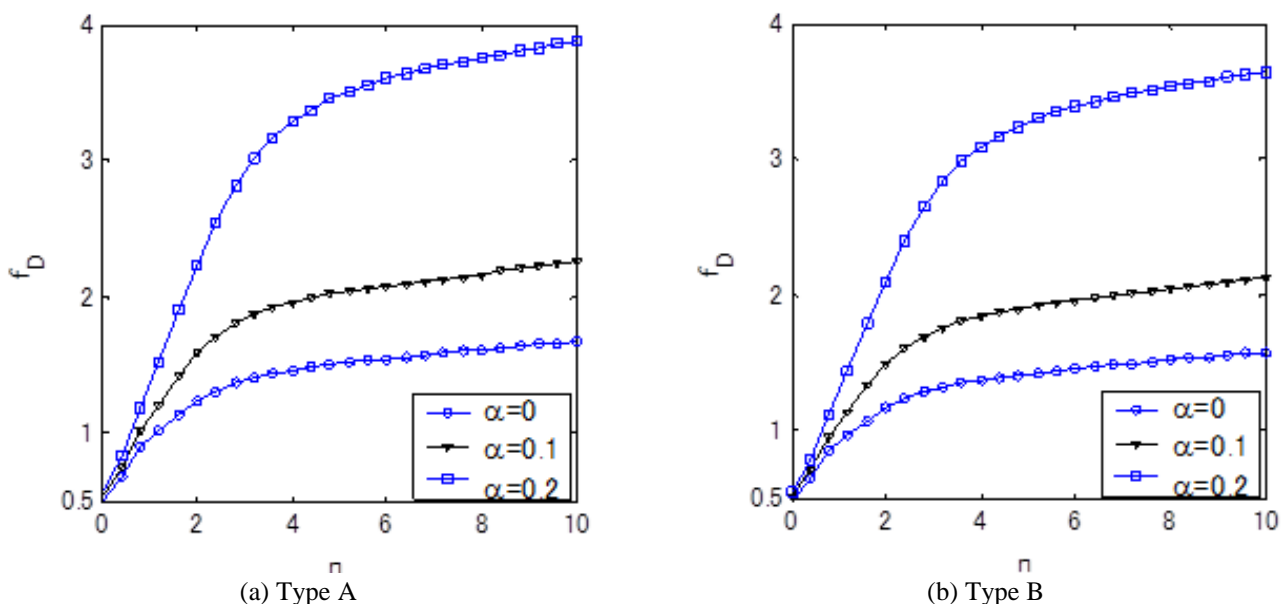


Fig. 7 The relation between DAF and index n of FG beam with different porosity volume fractions ($\beta=1, d=L/4, v=30$ m/s)

In Fig. 7, the relation between the DAF and the index n of the FG beam with $\beta=1$ is depicted for $v=30$ m/s, $d=L/4$ and various porosity volume fractions. Regardless of the index n and the section profile, the DAF increases as an increase of the porosity volume fraction, and this tendency is much more pronounced for the higher values of the index n . At a given value of the index n and porosity volume fraction α , the DAF of the type A beam is slightly higher than that of the type B beam. The obtained numerical results reveal that the porosity plays an important role in the dynamic response of FG beams, and it is necessary to take it into consideration for the dynamic analysis of FG beams under moving forces.

The effect of distance between moving forces on the mid-span deflection of FG porous beams is illustrated in Fig. 8 for $\alpha=0.1$, $\beta=0.5$, $n=5$ and $v=20$ m/s. An important role of the distance d between the moving forces on the dynamic response of the beam is clearly seen from the figure. The maximum mid-span deflection steadily decreases with an increase in the distance between the forces. The beam tends to execute more vibration cycles when the distance between the forces is larger. The decrease in the dynamic deflection by raising the distance between the forces can also be seen from Fig. 9, where the relation between the DAF and the moving speed v is illustrated for various values of the distance between the forces and for $n=5$, $\beta=0.5$, $\alpha=0.2$. Fig. 9 shows a remarkable decrease in the DAF by the increase in the distance between the forces, regardless of the moving speed and the section profile.

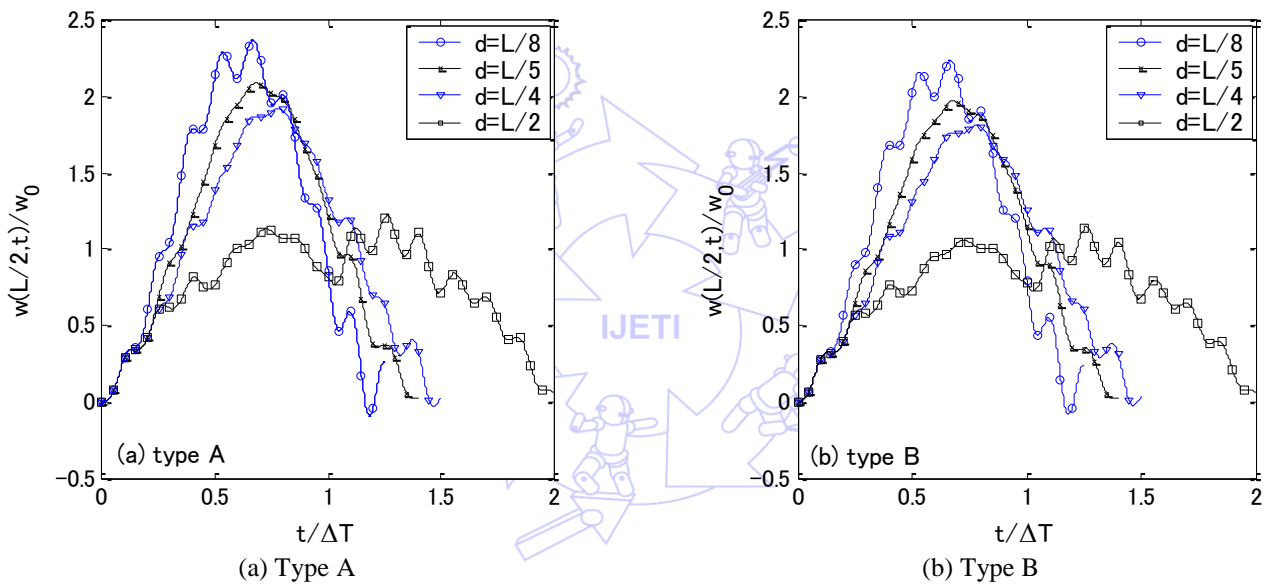


Fig. 8 Effect of distance between the forces on dynamic mid-span deflection ($\alpha=0.1$, $\beta=0.5$, $n=5$, $v=20$ m/s)

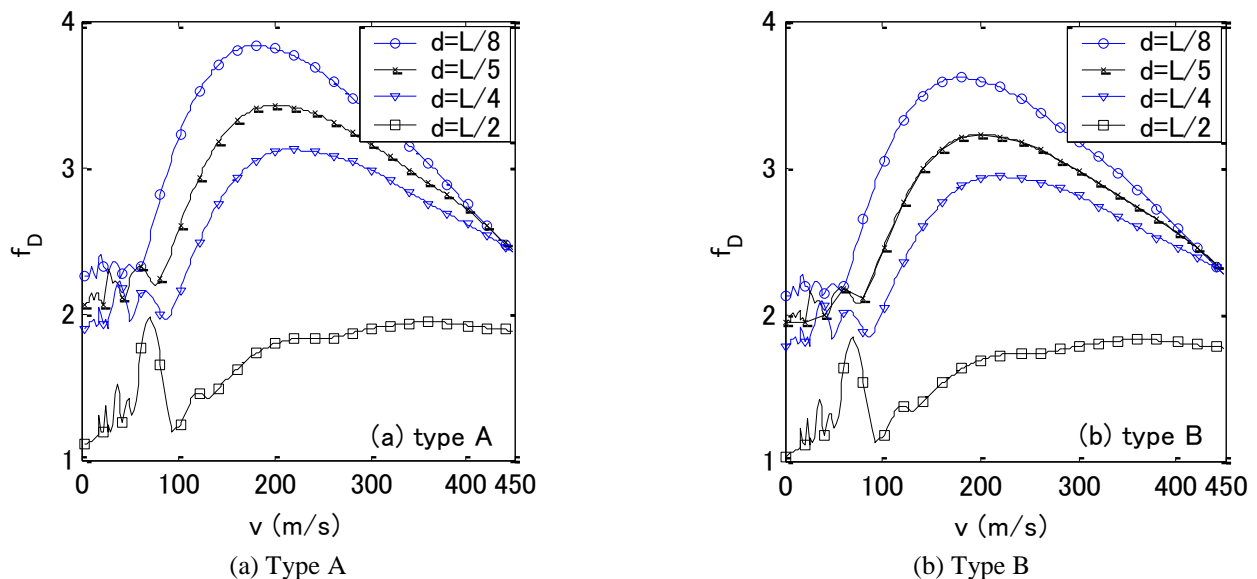


Fig. 9 The relation between DAF and moving speed with various distances between moving forces ($n=5$, $\beta=0.5$, $\alpha=0.2$)

Table 3 DAF with various values of section parameter β and index n ($\alpha=0.1, v=20$ m/s, $d=L/4$)

n	Type A beam				Type B beam			
	$\beta=0$	$\beta=0.5$	$\beta=1$	$\beta=1.5$	$\beta=0$	$\beta=0.5$	$\beta=1$	$\beta=1.5$
0.2	0.5836	0.6297	0.6914	0.7812	0.5836	0.5927	0.6028	0.6140
0.5	0.7547	0.8132	0.8884	0.9989	0.7547	0.7663	0.7788	0.7924
1	1.0790	1.1657	1.2826	1.4565	1.0790	1.0963	1.1155	1.1371
3	1.6632	1.7925	1.9557	2.1750	1.6632	1.6891	1.7170	1.7470
5	1.7881	1.9266	2.1015	2.3441	1.7881	1.8158	1.8455	1.8775
10	1.9509	2.1056	2.3126	2.6204	1.9509	1.9816	2.0154	2.0531

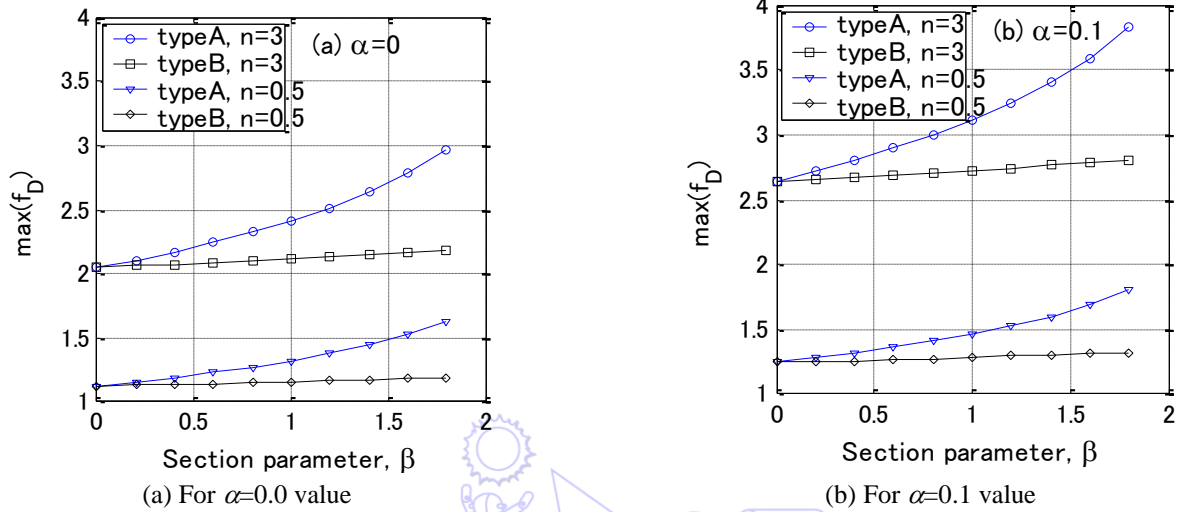


Fig. 10 Section parameter versus maximum dynamic amplification factor of nonuniform FG porous beam

The DAF of the FG porous beam with $\alpha=0.1$ is listed in Table 3 for $v=20$ m/s and $d=L/4$ and various values of the index n and section parameter β . As expected, the DAF steadily increases by raising the section parameter β , regardless of the index n and the section profile. By examining the table in more detail, one can see that the increase in the DAF by increase in the section parameter of the type A beam is much faster than that of the type B beam. For example, an increase of 23.53% when raising β from 0 to 1.5 is seen for the type A beam with an index $n=3$, while this value is just 4.80% of the type B beam with the same grading index. The effect of the section parameter on the dynamic response of the beam can also be seen from Fig. 10, where the maximum DAF is plotted as a function of the section parameter β for $\alpha=0$ and $\alpha=0.1$. As seen from the figure, comparing to the type B beam, the type A beam is much more sensitive to the change in the section parameter, regardless of the grading index n and the porosity volume fraction α . The porosity volume fraction considerably changes the maximum dynamic amplification deflection factor, but it hardly alters the relation between the maximum value of this factor and the section parameter.

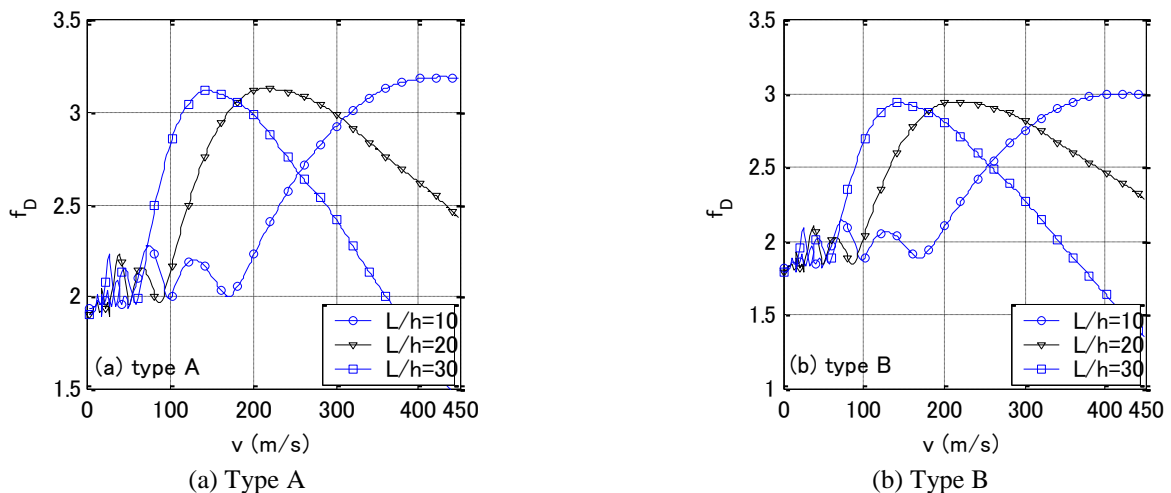


Fig. 11 Relation between DAF and moving speed for different aspect ratios ($n=5, \alpha=0.1, \beta=0.5, d=L/4$)

In order to study the effect of the aspect ratio on the dynamic response, the relation between the DAF and the moving speed of the beam with different aspect ratios, namely $L/h=10$, $L/h=20$ and $L/h=30$, is computed and the results are displayed in Fig. 11 for both two types of the section profile and $n=5$. As seen from the figure, the maximum DAF attains at a much higher moving speed for the beam having a smaller value of the aspect ratio. Also, the range of the moving speeds in which the DAF repeatedly increases and decreases is remarkably wider for the beam having a lower aspect ratio. This is because the fundamental frequency of the beam with the lower aspect ratio is higher, and this leads to the higher critical speed of this beam. The maximum DAF is slightly higher for the beam with a lower aspect ratio.

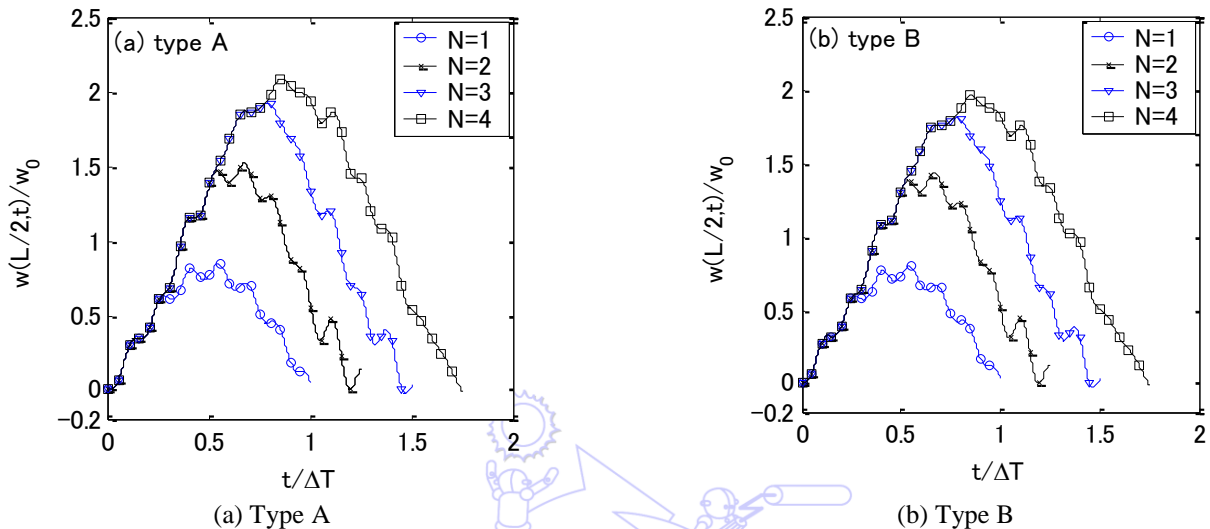


Fig. 12 Dynamic mid-span deflection of FG porous beam traversed by different number of forces ($n=5, \alpha=0.1, \beta=0.5, v=20$ m/s, $d=L/4$)

Finally, the effect of some the moving forces in the dynamic response of the FG porous beam is investigated. In Fig. 12, the dynamic mid-span deflection of the beam traversed by a different number of the forces is shown for $n=5, \alpha=0.1, \beta=0.5, v=20$ m/s and $d=L/4$. For $t \leq \Delta T/4$, all the curves in Fig. 12 are identical because the beam is under the action of only one force during this period. The number of the moving forces clearly affects the dynamic response of the beam, in which not only the mid-span deflection but also the time at which the maximum deflection occurred increases by the increase in the number of the forces. The relation between the DAF and the moving speed v , as depicted in Fig. 13 for $n=5, \alpha=0.1, \beta=0.5$ and $d=L/4$, also clearly shows the effect of the number of moving forces on the dynamic response of the beam. The moving speed at which the deflection factor reaches a peak, as clearly seen from Fig.13, is much higher when the beam traversed by some the forces.

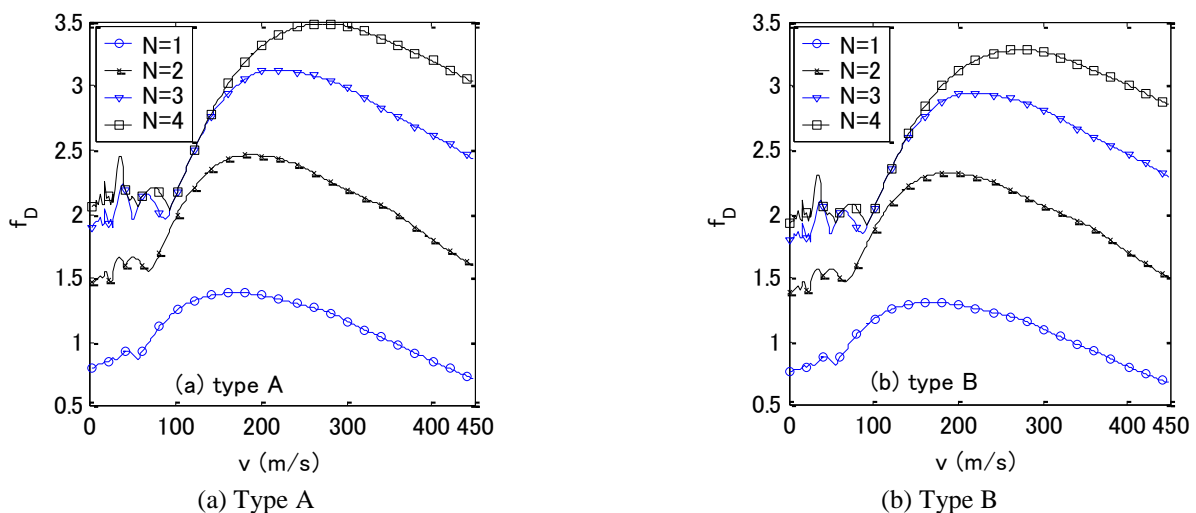


Fig. 13 Relation between DAF and moving speed for different number of forces ($n=5, \alpha=0.1, \beta=0.5, d=L/4$)

5. Conclusions

The dynamic response of nonuniform FG porous beams subjected to moving forces has been investigated in the present paper. A modified rule of mixture, taking the effect of the porosities into account, was adopted in evaluating the effective material properties. Based on Timoshenko beam theory, the equations of motion for the beams were derived from Hamilton's principle and solved by a finite element model. The dynamic response of a simply supported FG porous beam was computed by using the Newmark method. A parametric study was carried out to illustrate the effect of the material composition, aspect ratio and the loading parameters on the dynamic behaviour of the beams. The numerical results reveal that the porosity volume fraction, which has been taken into account in the present work, plays an important role in the dynamic response of the beam, and it is necessary to take the effect of porosities into consideration in the vibration analysis of FG beams traversed by moving forces.

Acknowledgement

This research is funded by Vietnam National Foundation for Science and Technology (NAFOSTED) under grant number 107.02-2015.02.

References

- [1] L. Frýba, *Vibration of solids and structures under moving loads*, 3rd ed. Prague: Thomas Telford House, 1999.
- [2] W. H. Lin and M. W. Trethewey, "Finite element analysis of elastic beams subjected to moving dynamic loads," *Journal of Sound and Vibration*, vol. 136, no. 2, pp. 323-342, January 1990.
- [3] D. Thambiratnam and Y. Zhuge, "Dynamic analysis of beams on elastic foundation subjected to moving loads." *Journal of Sound and Vibration*, vol. 198, no. 2, pp. 149-169, November 1996.
- [4] S. Ziaei-Rad, A. Ariaei, and M. Imregun, "Vibration analysis of Timoshenko beams under uniform partially distributed moving masses," *Proc. of the Institution of Mechanical Engineers, Part K: Journal of Multi-body Dynamics*, vol. 221, no. 4, pp. 551-566, December 2007.
- [5] M. Moghaddas, R. Sedaghati, and E. Esmailzadeh, "Finite element analysis of a Timoshenko beam traversed by a moving vehicle," *Proceedings of the Institution of Mechanical Engineers, Part K: Journal of Multi-body Dynamics*, vol. 223, no. 3, pp. 231-243, September 2009.
- [6] M. Moghaddas, E. Esmailzadeh, R. Sedaghati, and P. Khosravi, "Vibration control of Timoshenko beam traversed by moving vehicle using optimized tuned mass damper," *Journal of Vibration and Control*, vol. 18, no. 6, pp. 757-773, May 2012.
- [7] D. Roshandel, M. Mofid, and A. Ghannadiasl, "Dynamic response of a non-uniform Timoshenko beam, subjected to moving mass," *Proceedings of the Institution of Mechanical Engineers, Part C: Journal of Mechanical Engineering Science*, vol. 229, no. 14, pp. 2499-2513, October 2015.
- [8] M. Koizumi, "FGM activities in Japan," *Composites Part B: Engineering*, vol. 28, no. 1-2, pp. 1-4, 1997.
- [9] D. K. Jha, T. Kant, and R.K. Singh, "A critical review of recent research on functionally graded plates," *Composite Structures*, vol. 96, pp. 833-849, 2013.
- [10] A. Chakraborty, S. Gopalakrishnan, and J. N. Reddy, "A new beam finite element for the analysis of functionally graded materials," *International Journal of Mechanical Science*, vol. 45, no. 3, pp. 519-539, March 2003.
- [11] R. Kadoli, K. Akhtar, and N. Ganesan, "Static analysis of functionally graded beams using higher order shear deformation beam theory," *Applied Mathematical Modelling*, vol. 32, no. 12, pp. 2509-2525, December 2008.
- [12] A. E. Alshorbagy, M. A. Eltaher, and F. F. Mahmoud, "Free vibration characteristics of a functionally graded beam by finite element method," *Applied Mathematical Modelling*, vol. 35, no. 1, pp. 412-425, January 2011.
- [13] A. Shahba, R. Attarnejad, M. T. Marvi, and S. Hajilar, "Free vibration and stability analysis of axially functionally graded tapered Timoshenko beams with classical and non-classical boundary conditions," *Composites Part B: Engineering*, vol. 42, no. 4, pp. 801-808, June 2011.
- [14] D. K. Nguyen, "Large displacement response of tapered cantilever beams made of axially functionally graded material," *Composites Part B: Engineering*, vol. 55, pp. 298-305, December 2013.
- [15] D. K. Nguyen, "Large displacement behaviour of tapered cantilever Euler-Bernoulli beams made of functionally graded material," *Applied Mathematics and Computation*, vol. 237, pp. 340-355, June 2014

- [16] D. K. Nguyen and B. S. Gan, "Large deflections of tapered functionally graded beams subjected to end forces," *Applied Mathematical Modelling*, vol. 38, pp. 3054-3066, June 2014.
- [17] M. Şimşek and T. Kocatürk, "Free and forced vibration of a functionally graded beam subjected to a concentrated moving harmonic load," *Composite Structures*, vol. 90, no. 4, pp. 465-473, October 2009.
- [18] M. Şimşek, "Vibration analysis of a functionally graded beam under a moving mass by using different beam theories," *Composite Structures*, vol. 92, no. 4, pp. 904-917, March 2010.
- [19] M. Şimşek, "Non-linear vibration analysis of a functionally graded Timoshenko beam under action of a moving harmonic load," *Composite Structures*, vol. 92, no. 10, pp. 2532-2546, September 2010.
- [20] S. M. R. Khalili, A. A. Jafari, and S. A. Eftekhari, "A mixed Ritz-DQ method for forced vibration of functionally graded beams carrying moving loads," *Composite Structures*, vol. 92, no. 10, pp. 2497-2511, September 2010.
- [21] K. Rajabi, M. H. Kargarnovin, and M. Gharini, "Dynamic analysis of a functionally graded simply supported Euler-Bernoulli beam to a moving oscillator," *Acta Mechanica*, vol. 224, pp. 425-446, February 2013.
- [22] D. K. Nguyen, B. S. Gan, and T. H. Le, "Dynamic response of non-uniform functionally graded beams subjected to a variable speed moving load," *Journal of Computational Science and Technology (JSME)*, vol. 7, no. 1, pp. 12-27, January 2013.
- [23] T. H. Le, B. S. Gan, T. H. Trinh, and D. K. Nguyen, "Finite element analysis of multi-span functionally graded beams under a moving harmonic load," *Mechanical Engineering Journal (JSME)*, vol. 1, no. 3, pp. 1-13, June 2014.
- [24] B. S. Gan, T. H. Trinh, T. H. Le, and D. K. Nguyen, "Dynamic response of non-uniform Timoshenko beams made of axially FGM subjected to multiple moving point loads," *Structural Engineering and Mechanics*, vol. 53, no. 5, pp. 981-995, March 2015.
- [25] N. Wattanasakulpong and V. Ungbhakorn, "Linear and nonlinear vibration analysis of elastically restrained ends FGM beams with porosities," *Aerospace Science and Technology*, vol. 32, no. 1, pp. 111-120, January 2014.
- [26] N. Wattanasakulpong and A. Chaikittiratana, "Flexural vibration of imperfect functionally graded beams based on Timoshenko beam theory: Chebyshev collocation method," *Meccanica*, vol. 50, no. 5, pp. 1331-1342, May 2015.
- [27] D. Chen, J. Yang and S. Kitipornchai, "Elastic buckling and static bending of shear deformable functionally graded porous beam," *Composite Structures*, vol. 133, pp. 54-61, December 2015.
- [28] H. A. Atmane, A. Tounsi, and F. Bernard, "Effect of thickness stretching and porosity on mechanical response of a functionally graded beams resting on elastic foundations," *International Journal of Mechanics and Materials in Design*, pp. 1-14, July 2015.
- [29] F. Ebrahimi and M. Zia, "Large amplitude nonlinear vibration analysis of functionally graded Timoshenko beams with porosities," *Acta Astronautica*, vol. 116, pp. 117-125, November 2015.
- [30] F. Ebrahimi, F. Ghasemi, and E. Salari, "Investigating thermal effects on vibration behavior of temperature-dependent compositionally graded Euler beams with porosities," *Meccanica*, vol. 51, no. 1, pp. 223-249, January 2016.
- [31] J. B. Kosmatka, "An improve two-node finite element for stability and natural frequencies of axial-loaded Timoshenko beams," *Computers & Structures*, vol. 57, no. 1, pp. 141-149, October 1995.
- [32] M. Géradin and D. Rixen, *Mechanical Vibrations: Theory and Application to Structural Dynamics*, 2nd ed. Chichester: John Willey & Sons, 1997.
- [33] K. Henchi, M. Fafard, G. Dhatt, and M. Talbot, "Dynamic behaviour of multi-span beams under moving loads," *Journal of Sound and Vibration*, vol. 199, no. 1, pp. 33-50, January 1997.
- [34] M. Olsson, "On the fundamental moving load problem," *Journal of Sound and Vibration*, vol. 145, no. 2, pp. 299-307, March 1991.